Sweet revenge - *Streptococcus pyogenes* showcases first example of immune evasion through specific IgG glycan hydrolysis

Andreas Naegeli[1], Eleni Bratanis[1], Christofer Karlsson[1], Oonagh Shannon[1], Raja Kalluru[1,2], Adam Linder[1], Johan Malmström[1], Mattias Collin[1,*]

1) Lund University, Faculty of Medicine, Department of Clinical Sciences, Division of Infection Medicine, Lund, Sweden

2) Current affiliation: Department of Pathology, Stanford University School of Medicine, Stanford, California, USA.

* to whom correspondence should be addressed: Division of Infection Medicine, Department of Clinical Sciences, Biomedical Center B14, Lund University, SE-221 84 Lund, mattias.collin@med.lu.se

Abstract

Streptococcus pyogenes (Group A streptococcus, GAS) is an important human pathogen responsible for a wide variety of diseases from uncomplicated tonsillitis to life-threatening invasive infections. GAS secretes EndoS, an endoglycosidase able to specifically cleave the conserved *N*-glycan on human IgG antibodies. *In vitro*, removal of this glycan impairs IgG effector functions but its relevance to GAS infection *in vivo* is unclear. Using targeted mass spectrometry, we were able to characterize the effects of EndoS on host IgG glycosylation during the course of natural infections in human patients. We found substantial IgG glycan hydrolysis locally at site of infection as well as systemically in the most severe cases. Using these findings we were able to set up appropriate model systems to demonstrate decreased resistance to phagocytic killing of GAS lacking EndoS *in vitro,* as well as decreased virulence in a mouse model of invasive infection. This study represents the first described example of specific bacterial IgG glycan hydrolysis during infection and highlights the importance of IgG glycan hydrolysis for streptococcal pathogenesis. We thereby offer new insights into the mechanism of immune evasion employed by this pathogen with clear implications for treatment of severe GAS infections and future efforts at vaccine development.

Introduction

Streptococcus pyogenes (group A streptococcus, GAS) is a human pathogen causing a diverse range of diseases. GAS can cause mild infections such as tonsillitis and impetigo but also severe diseases such as streptococcal toxic shock syndrome, necrotizing fasciitis, and erysipelas[1]. Furthermore, repeated and/or untreated GAS infections can trigger serious postinfectious immune-mediated disorders, including acute poststreptococcal glomerulonephritis, acute rheumatic fever, and rheumatic heart disease[1]. With a prevalence of at least 18 million severe cases, leading to approximately half a million deaths world wide annually as well as over 700 million annual cases of mild infections[2], GAS infections are a large public health burden.

Protective immunity towards GAS is generally poor and recurrent infections are not uncommon, especially in children[3]. This is despite the fact that most people do in fact raise an adaptive immune response and exhibit high titers of IgG antibodies towards different GAS antigens[4-7]. The reason for the lack of protection is not entirely understood but can in part be attributed to the large number of different GAS serotypes and the surface antigen variability this entails[8]. GAS is also able to counteract adaptive immunity by specifically impairing IgG function. This can be mediated by non-immune IgG binding to Fc binding proteins on the streptococcal surface such as the M and M-related proteins[9,10] or through specific degradation of the IgGs themselves. GAS secretes for example the IgG specific protease IdeS which is able to cleave the antibody in the hinge region, separating the antigen-binding Fabs from the effector function-promoting Fc region[11].

GAS is further able to degrade IgGs by secretion of the endoglycosidase EndoS. This enzyme cleaves the conserved Fc *N*-glycan from IgGs with great specificity[12] (Fig. 1a). This glycan is situated at the interaction surface between the IgG and Fc receptors[13,14] as well as the complement system[15] and is therefore ideally located to influence IgG effector function. While an antibody´s specificity is determined by the Fab regions, the Fc region determines which effector functions are elicited and the structure of the Fc glycan has been shown to be crucial in the regulation of this process[16]. For example, IgGs lacking core fucosylation exhibit increased affinity for FcγRIIIA and are therefore significantly more potent in eliciting antibody-dependent cellular cytotoxicity[17,18]. Furthermore, the degree of galactosylation of the Fc glycan influences an IgGs ability to activate the complement system[19]. Consequently, IgG antibodies lacking the Fc glycan fail to bind to most Fc receptors and are unable to

62 activate the complement system[20,21]. Despite the accumulating evidence that antibody glycans
63 are instrumental in regulating and fine tuning the immune response, very little is know about
64 the role of antibody glycosylation during infections and if it contributes to the outcome of
65 disease. However, recent high profile studies that have suggested that the IgG glycosylation
66 status influences whether HIV infection is controlled[22,24] and whether *Mycobacterium*
67 *tuberculosis* infection is active or latent[23].

68 Due to this functional importance of the Fc *N*-glycan, its hydrolysis by EndoS leads to
69 impaired IgG effector functions such as Fc receptor binding and complement activation *in*
70 *vitro*[20,24,25]. This would intuitively suggest a role for EndoS in evasion of adaptive immunity
71 through perturbation of protective IgG responses. However, studies on the influence of
72 EndoS on GAS pathogenesis have so far been few and inconclusive. They were unable to
73 demonstrate under which conditions EndoS is expressed and active and had to rely on
74 overexpression or addition of recombinant enzyme to manifest a virulence phenotype[25,26].
75 These efforts at elucidating the contribution of EndoS to GAS virulence have been hampered
76 by the difficulty of finding relevant model systems and the lack of a sensitive analytical
77 approach to quantify EndoS activity in complex systems[25,26] .

78 We therefore wanted to take a different approach by first characterizing the effect of EndoS
79 on the hosts IgG glycosylation *in vivo* during the course of natural GAS infections in human
80 patients and then use these results to set up relevant model system able to show how EndoS
81 affects the hosts IgG response and how this contributes to GAS virulence. This necessitates
82 an assay that is robust, specific, and sensitive enough to be able to quantify the glycosylation
83 state of IgG in complex patient samples. We chose to employ selected reaction monitoring
84 (SRM), a targeted mass spectrometry approach that is uniquely suitable for this type of
85 analysis as it allows for the quantification of predefined target molecules (such as the EndoS
86 reaction products) directly from highly complex samples. SRM is based on precursor peptide
87 ion selection, fragmentation through collision, and detection of selected peptide fragment
88 ions in a triple quadrupole mass spectrometer. Precursor/fragment pairs, so called transitions,
89 are chosen that are unique to the molecule to be detected (i.e. the EndoS reaction products)
90 and data is only acquired for these defined targets (for a review see Picotti et al.[27]). In
91 previous studies, proteins with concentrations as low as 300 ng/ml have been reliably
92 quantified out of crude human plasma preparations[28,29] and SRM has also been used
93 successfully for quantification of the different glycan structures on IgG directly from serum
94 samples[30].

95 We employed SRM-MS to quantitatively assess the EndoS-mediated IgG glycan hydrolysis
96 in samples from natural GAS infections in humans. We used these findings to set up relevant
97 *in vitro* assays and animal models in order to demonstrate the importance of EndoS-mediated
98 antibody modification in evasion of adaptive immunity and therefore GAS virulence.

99 Results

100 A TARGETED MASS SPECTROMETRY APPROACH FOR QUANTITATIVE ANALYSIS OF IGG GLYCAN
101 HYDROLYSIS

102 In order to assess the effect of EndoS on IgG glycosylation during streptococcal infections *in*
103 *vivo*, we first needed an assay powerful enough to allow us to quantify the EndoS reaction
104 products directly from very complex samples such as patient material (plasma, wound swabs
105 or throat swabs). Previous attempts at measuring EndoS activity relied on SDS-PAGE[31,32] or
106 analysis of released glycans by HPLC[33]. These methods lack sensitivity, specificity and/or
107 are ill suited for analysis of complex material. We therefore developed an SRM mass
108 spectrometry method to specifically quantify the amount of glycan-hydrolyzed IgGs (IgG_{GH}).
109 As EndoS cleaves within the chitobiose core of the IgG *N*-glycan (Fig. 1a), it leaves the
110 reducing end *N*-Acetylglucosamine (GlcNAc) residue attached to the protein[34] and leads to
111 the generation of a new IgG proteoform with a truncated glycan that is not detected in healthy
112 individuals[35,36]. Samples were digested with trypsin and the peptides were treated with α-
113 fucosidase to remove potential core fucosylations and end up with a single EndoS reaction
114 product per IgG subclass. We defined SRM transitions for the tryptic peptides containing the
115 glycosylation site of human IgG (IgG1: EEQYN(GlcNAc)STYR, IgG2:
116 EEQFN(GlcNAc)STFR, IgG3: EEQYN(GlcNAc)STFR IgG4: EEQFN(GlcNAc)STYR)
117 modified with a single *N*-linked GlcNAc residue. As the glycopeptides of IgG3 and IgG4
118 have the same precursor mass, we defined transitions that are in common and quantified both
119 peptides together. To assess total IgG levels, previously developed SRM assays for
120 quantification of each IgG subclass[37] were included. All the transitions are listed in Table S2.
121 To determine the absolute amounts of IgG and IgG_{GH}, we synthesized heavy-isotope labeled
122 standard peptides corresponding to the peptides we analyzed, which could be spiked into the
123 samples to act as internal standards (Fig. 1b). The method was calibrated using a defined
124 human standard serum (Fig. S1&2, Table S3) and validated by analyzing a set of human
125 blood plasma samples with defined amounts of IgG_{GH}. For method comparison, the same
126 samples were also analyzed by SDS-PAGE and *Lens culinaris* agglutinin (LCA) lectin blot

127 (Fig. 1cd). The SRM method exhibited better precision and accuracy as well as a much lower
128 detection limit. Especially for samples where the IgG_{GH} content was low, as might be
129 expected in clinical samples, the SRM method outperformed the SDS-PAGE assay. This
130 together with low sample requirements, a large dynamic range and high analytical precision
131 (Fig. S1, S2) made this method highly suitable for the analysis of complex patient materials.
132 With this, method development was complete and we could start measuring EndoS activity
133 during GAS infections *in vivo*.

134 IGG GLYCANS ARE HYDROLYZED DURING GAS TONSILLITIS

135 Tonsillitis is the most common form of GAS infection and is characterized by throat pain,
136 fever, tonsillar exudates and cervical lymph node adenopathy[1]. To study the effects of EndoS
137 on patient IgGs during such an infection, we obtained 59 throat swab samples from a total of
138 54 patients who sought medical attention for a sore throat (Fig. 2a). 26 of these were
139 diagnosed with GAS tonsillitis by rapid strep test and/or throat culture and were prescribed
140 oral antibiotics. The other 28 patients exhibited a negative strep test and throat culture;
141 therefore the infection was suspected to be viral and left untreated. 5 of the patients
142 diagnosed with GAS tonsillitis were willing to return after antibiotic treatment and an
143 additional throat swab was collected for each of these (Fig. 2a)

144 We used SRM mass spectrometry to quantitatively analyze the levels of IgGs as well as their
145 glycosylation status in these throat swab samples. We observed no difference between GAS-
146 positive and GAS-negative patients in total IgG content or in the distribution of the four IgG
147 subclasses (data not shown). However, the percentage of glycan-hydrolyzed IgGs was
148 significantly higher in the GAS tonsillitis group, with glycan hydrolysis approaching 80% in
149 one case (Fig. 2b, left panel). This was no longer detectable in any of the samples taken after
150 antibiotic treatment (Fig. 2b, right panel). Furthermore, IgG glycan hydrolysis could be
151 correlated to the grade of throat pain and the general malaise experienced by the patients as
152 well as their Centor scores (a clinical scoring system aimed at distinguishing GAS tonsillitis
153 from viral infections[38]) (Fig. 2c). Taken together, these results suggest that EndoS is
154 expressed and active during acute GAS tonsillitis, but its effects quickly disappear upon
155 therapeutic intervention.

156 IGG ANTIBODIES ARE DEGLYCOSYLATED SYSTEMICALLY DURING GAS INDUCED SEPSIS

157 Sepsis is a state of systemic inflammation in response to an infection and the worst case
158 scenario in GAS infections[1]. To address the effect of EndoS on patient IgG antibodies during

159 invasive GAS infection leading to sepsis, we collected blood plasma from 32 patients
160 suffering from sepsis of various degrees of severity as well as 12 healthy volunteers. 18
161 patients had confirmed GAS infections whereas the other 14 suffered from various other
162 bacterial infections (Fig. 3a, table S5). All the sepsis patients were ranked according to the
163 degree of severity of their condition (sepsis, severe sepsis or septic shock). We used our SRM
164 method to determine IgG levels and glycosylation state in blood plasma (Fig. 3b, table S5).
165 The total IgG levels were not significantly different between the groups (Fig. 3b) and no
166 appreciable amounts of glycan-hydrolyzed IgG could be detected in any of the plasma
167 samples from the control groups (healthy or non-GAS sepsis). The same was true for milder
168 cases of GAS induced sepsis. However, the plasma of 5 out of 6 GAS patients suffering from
169 septic shock contained significantly increased amounts of IgG_{GH} (up to 1 mg/ml in the most
170 severe case) (Fig. 3b).

171 As we observed large differences in IgG glycan hydrolysis, even among the septic shock
172 patients, we hypothesized that differential expression of EndoS among the different GAS
173 strains infecting these patients could account for part of the observed variance. We were able
174 to obtain 6 GAS isolates from the blood cultures of these patients and analyzed the ability of
175 these strains to secrete EndoS into the culture medium *in vitro*. 3 isolates from severe sepsis
176 patients and 3 from septic shock patients (Fig. 3c, patients 1, 2 and 3) could be obtained. The
177 strains exhibited a large variability in EndoS expression as well as different levels of
178 degradation of the EndoS protein. Strains secreting substantial amounts of EndoS and strains
179 secreting almost no EndoS could be found in both groups. However, the amount of EndoS
180 secreted by the isolates from the septic shock patients *in vitro* corresponded well with the
181 amount of glycan-hydrolyzed IgG found in the corresponding patient´s blood plasma. The
182 isolate from the patient with no detectable IgG glycan hydrolysis *in vivo* did not secrete
183 detectable amounts of EndoS *in vitro,* and conversely, the isolate from the patient with the
184 highest *in vivo* glycan hydrolysis secreted the most EndoS *in vitro*. The cysteine protease
185 SpeB is a secreted GAS virulence factor and has been shown to cleave the EndoS enzyme[39].
186 Strikingly, SpeB is absent from the culture supernatant of the GAS isolate from patient 3
187 (with the highest degree of plasma IgG glycan hydrolysis, Fig. 3b) and consequently EndoS
188 is largely intact.

189 The IgG glycan hydrolysis we observed in plasma reflects a systemic modification of IgG,
190 which, due to the abundance of the antibody in circulation, necessitates large amounts of IgG
191 to be deglycosylated to reach detectable levels. Locally, at site of infection, the effects of

192 EndoS on the IgG pool are likely to be much more pronounced. To test this, we obtained
193 wound swabs from the infected tissue taken during surgery from two of the sepsis patients
194 suffering from necrotizing fasciitis (patients 1 & 2). We analyzed them by SRM mass
195 spectrometry to determine the degree of IgG glycan hydrolysis and compared the results to
196 those previously obtained from analysis of plasma samples (Fig. 3d). The samples originated
197 from two of the patients whose GAS isolates we have analyzed for EndoS expression *in vitro*
198 (Fig. 3c, patients 1 & 2). One isolate did not secrete any detectable amounts (Fig. 3c, patient
199 1) whereas the other one exhibited high EndoS expression (Fig. 3c, patient 2). Accordingly,
200 two very different patterns of IgG glycan hydrolysis could be observed in these patients (Fig
201 3d). The first patient showed no detectable IgG glycan hydrolysis in plasma and only a minor
202 amount in the wound swab sample. The second patient on the other hand exhibited moderate
203 IgG glycan hydrolysis in plasma (~0.7 % hydrolyzed) and the amount of IgG_{GH} was
204 considerably higher in the wound swab sample from the same day (~30% hydrolyzed). This
205 was no longer detectable in a sample from the same site that was taken during a second
206 surgery the day after.

207 As we observed that local IgG glycan hydrolysis was transient, we wanted to determine how
208 long-lasting the EndoS-mediated perturbation of the systemic IgG pool was. To this end we
209 obtained further plasma samples taken throughout the treatment and recovery periods (until
210 12 days after admission) from the patient exhibiting the highest amount of IgG_{GH} in plasma
211 (Fig. 3b, patient 3). Shortly after admission (time point 2h), the patient presented with very
212 low total IgG levels (3.3 mg/ml) and a high degree of IgG glycan hydrolysis (1 mg/ml). The
213 patient was given intravenous immunoglobulin (IVIG) treatment, upon which the total IgG
214 levels quickly normalized but the concentration of IgG_{GH} stayed high throughout the
215 analyzed time interval and was still around 0.5 mg/ml at the 12 days end point (Fig. 3e).

216 Taken together, these results show that EndoS is expressed and active during acute GAS
217 infection *in vivo*. It is able to hydrolyze the glycans from a considerable portion of the IgG
218 pool locally at the site of infection (both in tonsillitis and necrotizing fasciitis) as well as
219 systemically in the most severe cases of GAS sepsis. This points towards an important role
220 for EndoS in evasion of the immune defenses by perturbation of the hosts IgG response.

221 ENDOS IS EXPRESSED DURING GROWTH IN SALIVA AND PROTECTS GAS FROM PHAGOCYTIC
222 KILLING

223 While we were able to show that substantial IgG glycan hydrolysis takes place during GAS
224 infections, the functional consequences of this process for GAS pathogenesis remained
225 unclear and needed to be studied using appropriate model systems. As EndoS activity was
226 measureable in the majority of samples from GAS tonsillitis patients, we attempted to set up
227 a simplified *in vitro* model reminiscent of the conditions GAS encounters on an inflamed
228 tonsil during such an infection. When GAS colonizes the throat it would encounter saliva, an
229 increasing amount of plasma proteins as inflammation leads to vascular leakage[37] and finally
230 phagocytic immune cells trying to eradicate the bacteria. To approximate these conditions,
231 we grew GAS strains 5448 and AP1 as well as their respective isogenic *ndoS* mutants in
232 sterile-filtered saliva supplemented with 5% serum and tested if EndoS would be expressed
233 and active by SDS-PAGE. Based on electrophoretic mobility and/or LCA reactivity, both
234 wild type strains but neither of the mutants were able to fully deglycosylate the IgG pool
235 under these conditions (Fig. 4a, Fig. S6). Strain AP1 further expressed IdeS[11] leading to
236 proteolytic cleavage of IgG hinge in the culture supernatant. This resulted in a population of
237 antibodies where the Fc glycans and at least one half of the heavy chains had been cleaved
238 (Fig. S6).

239 As IdeS and EndoS might be partially redundant and strain 5448 only secreted EndoS
240 without any detectable IdeS activity when grown in saliva, we used this strain to test the
241 resistance of wild type and *ndoS* mutant bacteria to phagocytic killing by human monocyte-
242 derived macrophages (MDMs) and human polymorphonucelar leukocytes (PMNs) under the
243 conditions described above. Deletion of the *ndoS* gene led to a small but significant increase
244 in killing of the bacteria by both MDMs and PMNs (Fig. 4bc) and addition of recombinant
245 EndoS reversed the phenotype. However, increased susceptibility to phagocytic killing was
246 only observed when the assay was performed in the presence of serum containing GAS-
247 specific IgGs (as determined by measuring the IgG response to streptococcal M1 protein by
248 ELISA (Fig. S5)). In the absence of specific IgGs both mutant and wild type exhibited similar
249 resistance to phagocytic killing. This indicates that EndoS confers increased resistance by
250 neutralizing specific IgGs directed towards the pathogen and prevents them from mediating
251 phagocytosis.

252 ENDOS MUTANT GAS ARE LESS VIRULENT IN A MOUSE MODEL OF INVASIVE GAS INFECTION

253 In order to study the role of EndoS in neutralization of GAS-specific IgGs in more detail and
254 determine its contribution to the outcome of streptococcal infection, we established a mouse
255 model. As IdeS has no discernible activity on relevant subclasses of murine IgG (IgG1 and
256 IgG2b)[40] we were able to use the more mouse-virulent strain AP1 for these experiments
257 without confounding the results. Wild type and *ndoS* mutant[34] GAS were used to infect
258 C57BL/6J mice subcutaneously and both local (skin) and systemic (plasma, spleen) samples
259 were taken at 48h post infection to determine bacterial loads as well as IgG glycan hydrolysis
260 by SRM mass spectrometry (Fig. 5a). An assay analogous to the one for human IgGs was
261 developed to quantify murine IgG1 levels and its glycosylation status (Fig. S5). As EndoS
262 does not exhibit any murine IgG subclass specificity[41], this can be used as an indicator for
263 overall IgG glycan hydrolysis. When mice were infected with a wild type GAS strain, IgG1
264 was almost completely deglycosylated locally and around 30% glycan hydrolysis was
265 observed systemically (Fig. 5b, S8). The animals exhibited a heterogeneous response to
266 infection, with greatly varying degrees of severity observed. Consequently the measured
267 levels of IgG glycan hydrolysis also showed a large variance. We therefore tried to correlate
268 IgG glycan hydrolysis and bacterial load in the skin samples and found almost perfect
269 correlation (Fig. S5). Mice infected with the *ndoS* mutant developed local and systemic signs
270 of infection to a similar degree but showed no detectable IgG glycan hydrolysis (Fig. 5b,
271 S7,8). This indicates that EndoS is expressed and active during such an infection but does not
272 confer any selective advantages under these naïve conditions.

273 As EndoS targets the adaptive immune response, its functional role during GAS infection is
274 most appropriately studied in the context of adaptive immunity. We therefore immunized
275 mice prior to infection through two injections with purified streptococcal M1 protein
276 combined with adjuvant. After an IgG response to M1 was confirmed, the mice were infected
277 subcutaneously and survival was monitored for 5 days (Fig. 5c). This immunization protocol
278 lead to a complete protection at an infectious dose of 2.5×10^5 cfu which could be overcome
279 by increasing the dose to 2×10^7 cfu (Fig. S9). The majority of mice infected with wild type
280 bacteria at that dose succumbed to the infection within 2-3 days. On the other hand, more
281 than 90% of the mice infected with *ndoS* mutant bacteria survived the infection with only
282 milder symptoms (Fig 5d, left). This profound difference in susceptibility to infection
283 between wild-type and mutant could not be observed in animals that were mock immunized

284 by injection of adjuvant only, where both groups showed a similarly high mortality (>90%,
285 Fig. 5d, right).

286 Discussion

287 IgG is a central molecule of the mammalian immune system. It provides a link between
288 adaptive and innate immunity by specifically binding to antigens presented by a pathogen
289 with its Fab regions and recruiting immune effectors with its Fc region. Which exact effector
290 functions are elicited is a highly regulated process that lets the immune system tune its
291 response to the pathogen in question and mediate different effector functions against for
292 example a gram-positive bacterium, a gram-negative bacterium or a virus. One determining
293 factor in this process is the nature of the IgG antibody itself; namely its subclass and the
294 structure of its Fc glycosylation.

295 We here present the first evidence of a pathogen exploiting this regulatory mechanism by
296 specifically altering IgG Fc glycosylation *in vivo* during the clinical course of an infection.
297 By implementing a targeted proteomics approach based on SRM-MS we were able to study
298 the effects of EndoS on IgG antibodies during natural infections in human patients. Using
299 SRM we were able to detect and absolutely quantify glycan-hydrolyzed IgGs in a subclass
300 specific manner directly from a variety of very complex patient samples. With only minimal
301 amounts of sample required and detection limits below 0.5 ng, this method is far superior to
302 any other techniques used to measure IgG glycan hydrolysis to date. With this, we were able
303 to quantitatively address the effects of EndoS on a patient IgG population during
304 streptococcal infections. While a slight preference of EndoS towards IgG1[42] has been
305 reported, we did not observe any subclass specificity in any of the patient samples (Table
306 S4,5). Locally, at the site of infection, the degree of IgG glycan hydrolysis was generally high
307 (up to nearly complete hydrolysis) but the effects were only transient, disappearing quickly
308 upon therapeutic intervention. This was true both for mild infections (tonsillitis) as well as
309 severe, invasive infections (necrotizing fasciitis). This indicates that at site of infection, IgG
310 is turned over quickly and constantly replenished from the circulation and IgG glycan
311 hydrolysis is only detectable as long as bacterial load is high and EndoS is continuously
312 secreted. Due to the much larger amount of IgG in circulation as compared to the infected
313 tissue and the increased dilution of the enzyme further away from the site of infection, effects
314 on the systemic IgG pool in circulation were much harder to detect and therefore rarer. Only
315 in the most severe cases of invasive infections (septic shock), could glycan hydrolysis be

316 observed systemically. This systemic IgG glycan hydrolysis was long lasting with
317 approximately half of the glycan-hydrolyzed IgGs still present after 12 days. A similarly slow
318 recovery of IgG glycosylation to normal levels was also observed when rabbits or mice were
319 injected with recombinant EndoS as an experimental treatment of autoimmunity[31,43].

320 In both of our patient sets, only a portion of the patient samples showed detectable levels of
321 IgG_{GH} (58% of tonsillitis patients locally and 28% of sepsis patients systemically). In part,
322 this might be due to some GAS isolates expressing only very low levels of EndoS (Fig. 3c).
323 *In vivo* glycan hydrolysis was not associated with *covRS* mutation or any specific *emm*-type.
324 Indeed we detected it in infections with at least different 8 different *emm*-types (Table S4,5).
325 All publicly available GAS genome sequences contain an *ndoS* or an *ndoS*-like gene[44], but
326 expression of the EndoS protein differs greatly between different GAS isolates. However, the
327 fact that IgG glycan hydrolysis correlates to disease severity both in tonsillitis and invasive
328 disease indicates that we – due to analytical limitations – might not be able to detect EndoS-
329 mediated IgG glycan hydrolysis in samples from patients suffering from less severe
330 infections. This is true especially for the GAS sepsis patient samples. Apart from two
331 exceptions, we were only able to study IgG in blood plasma and therefore were unable to
332 address potential perturbations of the local IgG pool at site of infection in more detail. Indeed
333 among the sickest patients in each cohort the percentage of samples with detectable IgG_{GH}
334 was considerably higher. 5 out of 6 GAS septic shock patients (83%) exhibited measureable
335 systemic IgG glycan hydrolysis and among the sickest half of the tonsillitis patients (based on
336 estimation of general malaise) glycan hydrolysis of the local IgG pool was detectable in all
337 but one patient (92% total). While studying the activity of EndoS during GAS tonsillitis, we
338 also observed a considerable amount of IgG glycan hydrolysis in some of our control samples.
339 We speculate that this was due to enzymatic activities of the oral micro flora, especially oral
340 streptococci which are known to express a large number of glycoside hydrolases[45]. This is
341 supported by the fact that IgG glycan hydrolysis was not detectable in any of the samples we
342 took after antibiotic treatment.

343 While we were able to show that IgG glycan hydrolysis takes place during GAS infection *in*
344 *vivo*, the functional consequences of this process could not be deduced directly from the
345 patient data. Removal of the Fc glycan by EndoS has previously been shown to impair both
346 Fc receptor interaction and complement activation *in vitro*[20,25]. While EndoS has been
347 speculated to contribute to GAS virulence, all studies showing this to date had to resort either
348 to addition of recombinant EndoS or overexpression[25,26] to see any effect. Thus, the

349 conditions under which endogenous EndoS is expressed, active and able to confer a selective
350 advantage to the bacteria remained unclear. EndoS expression is highly regulated and while
351 the regulatory network responsible remains obscured, it has been shown to involve both
352 transcriptional regulation by *ccpA* and weakly by *covR/S*[46] as well as posttranslational
353 regulation through proteolysis[47]. Transcriptomics studies have shown that EndoS expression
354 is repressed during growth in rich medium[48] (such as the standard Todd-Hewitt broth) and is
355 not induced until the bacteria reach stationary phase[49]. This means that most standard assays
356 used to study streptococcal virulence factors such as incubating log phase bacteria with
357 phagocytic cells and IgG (or the classic Lancefield assay[50]) are ill suited to address the role of
358 EndoS or similar secreted immunomodulatory activities. This might constitute a major
359 shortcoming in for example analysis of protective effects of IgGs in vaccination studies,
360 potentially resulting in overestimation of vaccine efficacy.

361 We used our characterization of IgG glycan hydrolysis *in vivo* to set up relevant model
362 systems to address the contribution of EndoS to GAS pathogenesis. Based on our findings on
363 IgG glycan hydrolysis during GAS tonsillitis, we were able to approximate the conditions
364 GAS encounters on an inflamed tonsil using human saliva and serum. This prompted wild
365 type bacteria to secrete enough EndoS to completely deglycosylate the IgGs present and
366 neutralize the contribution of GAS-specific IgGs to phagocytic killing by human
367 macrophages or neutrophils *in vitro*. *ndoS* mutant bacteria on the other hand were unable to
368 cleave the glycans from IgG and consequently exhibited a higher susceptibility to phagocytic
369 killing. This phenotype could be reversed by externally adding recombinant EndoS. These
370 results, together with the fact that the *ndoS* mutation had no phenotype in the absence of
371 GAS-specific IgGs indicates that the observed phenotype is due to deglycosylation of the
372 GAS-specific IgGs which in turn impairs their ability to mediate phagocytic killing. There
373 seems to be no general attenuation of the *ndoS* mutant, nor any benefits in glycan hydrolysis
374 of non-specific IgGs.

375 An animal model of local skin infection leading to invasive infection showed very similar
376 dynamics. Mice infected with *ndoS* mutant bacteria exhibited no IgG glycan hydrolysis and
377 were significantly less likely to die from the infection than mice infected with wild type GAS.
378 This difference was however only clearly evident in the context of adaptive immunity (i.e. in
379 animals that had been immunized against GAS prior to infection). In agreement with the
380 results from the phagocytosis assays and previous studies[26], naïve mice showed a very similar
381 susceptibility towards both wild type and *ndoS* mutant bacteria; with no significant

382 differences in survival, weight loss or bacterial load in the skin (Fig. 5, Fig. S7). Only the
383 bacterial burden in the spleen was slightly decreased in mice infected with *ndoS* mutant
384 bacteria (Fig. S7). This might point to a small degree of innate protection conferred by
385 natural IgGs[51] that can be counteracted by EndoS.

386 While not generally used to treat sepsis[52,53], administration of intravenous immunoglobulin
387 (IVIG) has shown promise as a treatment for streptococcal toxic shock syndrome[54,55] and
388 necrotizing fasciitis[56]. Its mode of action is thought to involve neutralization of bacterial
389 superantigens and inhibition of pro-inflammatory signaling[57-59]. Our data points to another
390 reason why IVIG treatment could improve the outcome of severe streptococcal infections.
391 EndoS-mediated glycan hydrolysis inactivates IgGs and as shown in this study, such antibody
392 modifications can be systemic, long lasting and affect a considerable fraction of the patient's
393 total IgG pool. GAS can lower functional IgG levels even further through secretion of the
394 IgG protease IdeS[11,37]. In such cases, IVIG in concert with antimicrobial therapy could help
395 to quickly normalize the level of functional IgG in circulation. We observed such an effect in
396 one patient (Fig. 3e, patient 3).

397 Despite an abundance of anti-GAS IgGs in the serum of most people[4-7], protective immunity
398 towards the pathogen does not ensue. Furthermore, development of effective GAS vaccines
399 has proven challenging. Herein we present a possible mechanism to explain why anti-GAS
400 IgGs often confer such poor protection: GAS is able to effectively neutralize the contribution
401 of IgG to host defense through specific degradation of the IgG antibodies. We have
402 demonstrated the dynamics of IgG glycan hydrolysis by EndoS in this study and a recent
403 study has also shown significant levels of IdeS-mediated IgG proteolysis during GAS
404 infections *in vivo*[37]. This makes GAS a very proficient evader of IgG-mediated immunity, a
405 fact that has implications for the treatment of severe GAS infections and has to be taken into
406 account in future research into the immune response to GAS as well as in the continuing
407 efforts at development of an effective vaccine against the pathogen. Finally, immune evasion
408 through modification of IgG glycosylation might not be restricted to GAS and enzymes
409 similar to EndoS can be found in many other pathogenic species such as *Enterococcus*
410 *faecalis*[60], *Streptococcus pneumoniae*[61] as well as other non-group A streptococci[62,63]. Indeed,
411 an EndoS homolog from *Streptococcus equi*[63] proved a protective antigen in a vaccination
412 trial in mice, pointing towards its importance for the infection process. Bacterial modulation
413 of IgG glycosylation might therefore be a more widespread phenomenon that warrants further
414 study.

415 # Materials and Methods

416 PATIENT SAMPLES

417 Tonsillar swabs (n = 54, ESwab Liquid Amies) were obtained from patients (>8 years old)
418 seeking clinical care because of a sore throat at the primary healthcare clinics at
419 Laurentiikliniken and Skåne University Hospital (SUS) both in Lund, Sweden. GAS
420 tonsillitis was diagnosed by rapid strep test (antigen detection) and routine bacterial culturing.
421 A follow-up tonsillar swab sample (3-5 days post) was taken from a subset of patients (n=5)
422 treated with antibiotics (Table S4). Wound swabs from the local infection site of patients
423 clinically diagnosed with GAS sepsis and necrotizing fasciitis were obtained from SUS, Lund
424 Sweden (n=4) during surgical intensive care (Table S5). Patient swab samples were
425 transported on dry ice before storage at -80 °C. The patient plasma samples were part of a
426 larger cohort collected at the Clinic for Infectious Diseases or at Intensive Care Unit at Lund
427 University Hospital between 2005 and 2015. All human samples were obtained with
428 informed consent and with the approval of the local ethics committee (see 'Ethical
429 Considerations' section below).

430 SAMPLE PREPARATION FOR MASS SPECTROMETRY

431 Proteins from the swab samples were extracted and homogenized in water using a bead-
432 beater (Fastprep-96, MP-Biomedicals). 0.625 µl plasma or 50 µg of protein from swabs or
433 skin homogenates were prepared for MS analysis using the SmartDigest Kit (Thermo
434 Scientific). Samples were denatured at 90°C followed by digestion for 3.5 hours at 70°C. The
435 peptides were reduced using 50 mM TCEP, alkylated with 100 mM iodoacetamide and
436 finally purified using SOLAµ HRP plates (Thermo Scientific). The peptide samples were
437 dried in a vacuum centrifuge and dissolved in 100 µl 50 mM sodium acetate buffer (pH 5)
438 containing 50 mU Thermatoga maritima α-fucosidase (Megazymes). After incubation at
439 70°C for 14 h, the samples were purified a second time on SOLAµ HRP plates and dried in a
440 vacuum centrifuge.

441 SRM MASS SPECTROMETRY

442 Peptide samples were dissolved in 2%ACN, 0.2% FA and AQUA peptides (Thermo
443 HeavyPeptide QuantPro, table S3) were spiked in. The amount of peptide standards was
444 adjusted so that the ratio of light to heavy signal falls within the interval of 0.1 to 10. Sample
445 corresponding to 1 µg of protein were analyzed by SRM mass spectrometry using a TSQ
446 Vantage triple quadrupole mass spectrometer coupled to an Easy-nLC II system (both

447 Thermo Scientific) equipped with a PicoChip column (PCH7515-105H354-FS25, New
448 Objective). Data was acquired with a spray voltage of 1500V, 0.7 FWHM on both
449 quadrupoles and a dwell time of 10ms. Assays for all the non-glycopeptides were obtained
450 from published studies [37,64] while glycopeptide assays were developed as described here[65].
451 Assay set-up, empirical collision energy optimization as well as data analysis was done using
452 Skyline [66,67]. The analyzed transitions are listed in table S2.

453 DETERMINATION OF DETECTION LIMITS

454 Human IgG subclass reference serum NOR-1 (NordicMUBio) was used to create standard
455 samples for method calibration and determination of detection limits. For a fully glycan
456 hydrolyzed sample, the serum was incubated with 50 µg/ml recombinant EndoS at 37°C for
457 16h. Both treated and untreated serum samples were prepared for mass spectrometry analysis
458 separately as described above. Peptides were dissolved in 2%ACN, 0.2% FA at a
459 concentration of 1 µg/µl and spiked with AQUA IgG glycopeptides. The EndoS-treated
460 sample was further spiked with AQUA IgG peptides. Three separate dilution series were
461 prepared by serially diluting the EndoS-treated sample with peptides from the untreated
462 sample. Finally, peptides samples corresponding to 1 µg of protein form each dilution were
463 analyzed by SRM mass spectrometry. From this data set detection limits for each peptide
464 were determined separately:

465 Limit of blank (LoB): $LoB = mean_{blank} + 1.645(SD_{blank})$ (1)

466 Limit of detection (LoD): $LoD = (LoB + 1.645(SD_{low\ concentration\ sample})$ (2)

467 Untreated samples were used to determine LoB according to formula 1. The first dilution
468 with a concentration above LoB was used as the low concentration sample for LoD
469 determination with formula 2. A lower limit of quantification (LLoQ) was defined as two
470 time LoD and in all further experiments, measured amounts below LLoQ were considered as
471 being 0. As the concentrations of all 4 IgG subclasses in serum NOR-1 have been determined
472 by the manufacturer, we could also use this dataset to calibrate the quantification and correct
473 for incomplete digestion and sample loss during preparation. For each data point above LOD
474 and with a light to heavy between 0.1 and 10 conversion factors were determined by dividing
475 the known IgG subclass concentrations with the measured light to heavy ratios. These
476 conversion factors were averaged (table S3) and are used to determine absolute amounts from
477 measured light to heavy ratios in all further experiments with human samples. The same
478 procedure was followed when the assay for murine IgG1 was developed. The standard

479 sample there was a monoclonal mouse IgG1 (MA-69, Biolegend, San Diego, USA) that was
480 treated with recombinant EndoS and spiked into human plasma as a background proteome.

481 SDS-PAGE AND LECTIN BLOT

482 IgG was purified using Protein G (Ab SpinTrap, GE Healthcare). Samples were separated on
483 SDS-PAGE (Mini-protean TGX stainfree gels, 4-15% acrylamide, BioRad), imaged using a
484 ChemiDoc MP imaging system (BioRad) and transferred to low fluorescent PVDF
485 membranes using the Transblot Turbo kit (BioRad). Membranes were blocked for 1h in lectin
486 buffer (10 mM HEPES pH7.5, 150 mM NaCl, 0.01 mM $MnCl_2$, 0.1 mM $CaCl_2$, 0.1% (v/v)
487 tween 20) followed by incubation with 5 µg/ml fluorescein-labeled LCA lectin (Vector
488 laboratories). After extensive washing in lectin buffer, the membranes were imaged using a
489 ChemiDoc MP imaging system (BioRad).

490 ANALYSIS OF ENDOS AND SPEB EXPRESSION *IN VITRO*

491 AP1, AP1ΔndoS, AP1ΔspeB and the GAS clinical isolates were grown overnight at 37°C,
492 5% CO_2 in C-medium (0.5% (w/v) Proteose Peptone No. 2 (Difco) and 1.5% (w/v) yeast
493 extract (Oxoid) dissolved in CM buffer (10 mM K_2PO_4, 0.4 mM $MgSO_4$, 17 mM NaCl
494 pH 7.5). The cultures were pelleted and the supernatants sterile filtered (Millex-GP filter unit
495 0.22µm, Millipore). Proteins were precipitated from the supernatants with 5% TCA
496 (trichloroacetic acid) and analyzed by SDS-PAGE under reducing conditions. Proteins were
497 transferred to PVDF-membranes using the Trans-Blot Turbo equipment (Bio-Rad
498 Laboratories) according to manufacturer's instructions. Membranes were blocked with 5%
499 (w/v) blotting-grade blocker (Bio-Rad Laboratories) in PBST, followed by incubation with
500 EndoS or SpeB rabbit antiserum [12,68] another wash and incubation with a secondary antibody
501 (goat anti-rabbit HRP-conjugated antibody, BioRad). The membranes were developed using
502 Clarity Western ECL substrate (BioRad) and visualized with a ChemiDoc MP Imager (Bio-
503 Rad, USA).

504 ANALYSIS OF *EMM* AND *COVRS* SEQUENCES

505 *emm* sequences of the GAS clinical isolates were analyzed according to protocols published
506 by the CDC and compared to a database of known *emm* sequences using the tool on the CDC
507 website (https://www2a.cdc.gov/ncidod/biotech/strepblast.asp). The *covRS* operon was
508 sequenced as previously described[69] and compared to published sequences of the same
509 serotype.

510 *IN VITRO* TONSILLITIS MODEL

511 *Preparation of saliva:* Saliva from healthy volunteers was collected in the morning after
512 extensive brushing of the teeth. The saliva was centrifuged (20 min, 20000 g), sterile filtered
513 (Steriflip GP 0.22 µm, Milipore) and either used directly or kept at -20°C until use.

514 *Preparation of polymorphonuclear leukocytes (PMNs)*: 20 ml blood was collected into
515 EDTA blood collection tubes (BD Bioscience) and the PMNs were isolated using
516 PolyMorphPrep (Axis-shield) according to manufacturers recommendations. After counting,
517 the cells were diluted into RPMI medium and seeded at 50000 cells/well into a 96-well plate.

518 *Preparation of monocyte derived macrophages (MDMs)*:

519 Peripheral blood mononuclear cells (PBMCs) were isolated from leukocytes of healthy
520 anonymous donors provided by the Lund University Hospital. Red blood cells were removed
521 by centrifugation on Lymphoprep (Fresenius Norge As, Oslo, Norway) and recovered
522 PBMCs were washed to remove platelets. Monocytes were isolated using a magnetic cell
523 separation system with anti-CD14 mAb-coated microbeads (Miltenyi Biotec). CD14-positive
524 monocytes were seeded into 12 well plates at 5×10^5 cells/well and differentiated into
525 macrophages by culture in complete RPMI 1640 medium (Gibco) supplemented with 10%
526 heat-inactivated human AB+ serum, 50 nM β-mercaptoethanol (GIBCO), Penicillin-
527 Streptomycin (Sigma) and 40 ng/ml M-CSF (Peprotech) at 37°C under a humidified 5% CO2
528 atmosphere for 6 days. Medium was replaced on day 2 and on day 4, when cells were washed
529 with PBS and the medium was replaced with antibiotic-fee medium. The cells were further
530 incubated until day 6 when the infection experiments took place.

531 *Killing assays:* GAS 5448 and an isogenic *ndoS* mutant[26] were grown overnight in THY
532 medium at 37°C, 5% CO_2, diluted 1:10 into fresh medium and let grow to mid-log phase (OD
533 = 0.4). Cultures were diluted 1:50 into 1 ml of saliva, incubated for 2h at 37°C, 5% CO_2 and
534 diluted again (1:20) into 1 ml fresh saliva (supplemented with 5% serum and 0.5 µg/ml
535 recombinant EndoS where suitable). After 20h at 37°C, 5% CO_2 the bacteria were diluted
536 1:10 into RPMI medium and used to infect PMNs or MDMs at an MOI of 2. After 30min (for
537 PMNs) or 2 h (for MDMs) incubation at 37°C, 5% CO_2 the cells were lysed using ddH2O
538 (for PMNs) or 0.025% Triton X-100 (for MDMs) and the number of surviving bacteria was
539 determined by plating on THY agar plates.

540 ANALYSIS OF ENDOS EXPRESSION *IN VITRO*

541 AP1, the *ndoS* mutant and the GAS clinical isolates were grown in C-medium (37°C and 5%
542 CO2) overnight and normalized to the same OD_{620} using fresh C-medium. Bacteria were
543 pelleted by centrifugation and the supernatants filtered (Millex-GP filter unit 0.22µm,
544 Millipore). Proteins were precipitated from the supernatants with 5% TCA (trichloroacetic
545 acid) and analyzed by SDS-PAGE under reducing conditions. Proteins were transferred to
546 PVDF-membranes using the Trans-Blot Turbo kit (Bio-Rad Laboratories) according to
547 manufacturer's instructions. Membranes were blocked with 5% (w/v) blotting-grade blocker
548 (Bio-Rad Laboratories) in PBST, followed by incubation with EndoS[34] or SpeB[68] antiserum
549 The membranes were washed followed by incubation with a secondary antibody (goat anti-
550 rabbit HRP-conjugated antibody, BioRad). The membranes were developed using Clarity
551 Western ECL substrate (BioRad) and visualized with a ChemiDoc MP Imager (Bio-Rad,
552 USA).

553 MOUSE INFECTIONS:

554 *Acute infection model of GAS in naïve C57BL/6J mice* GAS AP1 and *ndoS* mutant (Table S1)
555 were grown to logarithmic phase in Todd–Hewitt broth (37°C, 5% CO_2). Bacteria were
556 washed and resuspended in sterile PBS. 2-3x10^5 cfu of AP1 (n=13) or *ndoS* mutant (n=13)
557 were injected subcutaneously into the flank of 9-week-old female C57BL/6J mice (Scanbur/
558 Charles River Laboratories). Control mice were injected with PBS (n=8). Mice were
559 rehydrated subcutaneously with saline at 24 h post infection. Body weight and general
560 symptoms of infection were monitored regularly. Mice were sacrificed at 48 h post infection
561 and organs (blood, spleens and skin) were harvested to determine the degree of bacterial
562 dissemination and IgG glycan hydrolysis.

563 *M1 immunization and survival study* 9-week-old female C57BL/6J mice (Scanbur/ Charles
564 River Laboratories) were injected subcutaneously with M1 protein on days 0 and 21 (10
565 µg/dose), purified as previously described[68,71]. The protein was administered as a 50:50
566 solution of M1:adjuvant (TiterMax Gold), in a 50 µl volume. Control mice were similarly
567 injected with PBS:adjuvant solution. Serum was collected at day 49 and anti-M1 titers were
568 measured by ELISA as previously described[72] with a goat anti-mouse HRP-conjugated
569 secondary antibody at 1:5000 (BioRad). Immunized and control mice were infected
570 subcutaneously into the flank with 2x10^7 cfu of the AP1 (n=17) or *ndoS* mutant (n=12) at day
571 56. Mice were rehydrated subcutaneously with saline 24 h post infection. Weight and general

572 symptoms of infection were monitored every 12 h during the acute phase of the infection, and
573 then every 24 h until termination of the study at 5 days post infection. Animals displaying a
574 weight loss exceeding 20% (until 72 h post infection) or 15% (after 72 h post infection) were
575 considered moribund and sacrificed.

576 STATISTICS

577 All statistical analyses were preformed using GraphPad Prism 7. Phagocytic killing assays
578 were analyzed using one-way ANOVA followed by Tukey´s multiple comparison test. IgG
579 hydrolysis data was analyzed using a Mann-Whitney test or a Kruskal-Wallis test in
580 combination with Dunn´s multiple comparison test (when more than two datasets were
581 compared). Correlation was determined according to Spearman and survival data was
582 analyzed using a Mantle-Cox test.

583 ETHICAL CONSIDERATIONS

584 All animal use and procedures were approved by the local Malmö/Lund Institutional Animal
585 Care and Use Committee, ethical permit number M115-13. Collection and analysis of human
586 throat swabs and plasma samples was approved by the local ethics committee (dnr 2005/790,
587 2015/314 and 2016/39).

588 AUTHOR CONTRIBUTIONS

589 AN designed the study, performed all mass spectrometry and phagocytosis experiments and
590 wrote the manuscript. EB and OS designed and performed all animal experiments. CK helped
591 with SRM assay development and data analysis. AL organized and supervised collection of
592 clinical samples. RK prepared cells for phagocytosis experiments. JM and MC designed the
593 study, supervised the research, and wrote the manuscript.

594 DATA AVAILABILITY

595 The MS analysis files from Skyline underlying figures 1d, 2b, 3bde and 5b are available on
596 PanoramaWeb (https://panoramaweb.org/endos.url). The MS raw data is available upon
597 request.

598 ACKNOWLEDGEMENTS

599 We thank Fanny Olsson Byrlind and Tomas Lindgren for help with collection of patient
600 samples, Bo Nilsson for collecting the GAS clinical isolates, and Fredric Carlsson for helpful
601 discussions about the choice of animal model. This work was supported by grants to AN
602 from the Swiss National Science Foundation (P2EZP3_155594 and P300PA_167754), the

603 Royal Physiographic Society in Lund and the Sigurd and Elsa Goljes Memorial Foundation.
604 This work was further supported by grants to MC from the Swedish Research Council
605 (projects 2012-1875 and 2017-02147), the Royal Physiographic Society in Lund, the
606 Foundations of Åke Wiberg, Alfred Österlund, Gyllenstierna-Krapperup, Torsten Söderberg,
607 the King Gustaf V`s 80 years fund, and Hansa Medical AB as well as grants to JM from
608 Foundation of Knut and Alice Wallenberg (2016.0023), European research council starting
609 grant (ERC-2012-StG-309831), the Swedish Research Council (project 2015-02481), the
610 Wallenberg Academy Fellow program KAW (2012.0178 and 2017.0271), Olle Engkvist
611 Byggmästare and the Medical Faculty of Lund University. The funders had no role in
612 preparation of the manuscript or in the decision to publish

613 # References

614 1. Walker, M. J. *et al.* Disease manifestations and pathogenic mechanisms of group a
615 Streptococcus. *Clin. Microbiol. Rev.* **27,** 264–301 (2014).
616 2. Carapetis, J. R., Steer, A. C., Mulholland, E. K. & Weber, M. The global burden of
617 group A streptococcal diseases. *Lancet Infect. Dis.* **5,** 685–694 (2005).
618 3. St Sauver, J. L., Weaver, A. L., Orvidas, L. J., Jacobson, R. M. & Jacobsen, S. J.
619 Population-based prevalence of repeated group A beta-hemolytic streptococcal
620 pharyngitis episodes. *Mayo Clin. Proc.* **81,** 1172–1176 (2006).
621 4. Lancefield, R. C. Current knowledge of type-specific M antigens of group A
622 streptococci. *J. Immunol.* **89,** 307–313 (1962).
623 5. Todd, E. W. Antigenic Streptococcal hemolysin. *J. Exp. Med.* **55,** 267–280 (1932).
624 6. Åkesson, P. *et al.* Low antibody levels against cell wall-attached proteins of
625 *Streptococcus pyogenes* predispose for severe invasive disease. *J. Infect. Dis.* **189,**
626 797–804 (2004).
627 7. O'Connor, S. P. *et al.* The human antibody response to streptococcal C5a peptidase. *J.*
628 *Infect. Dis.* **163,** 109–116 (1991).
629 8. McMillan, D. J. *et al.* Updated model of group A Streptococcus M proteins based on a
630 comprehensive worldwide study. *Clin. Microbiol. Rev.* **19,** E222–9 (2013).
631 9. Åkesson, P., Schmidt, K. H., Cooney, J. & Björck, L. M1 protein and protein H:
632 IgGFc- and albumin-binding streptococcal surface proteins encoded by adjacent genes.
633 *Biochem. J.* **300 (Pt 3),** 877–886 (1994).
634 10. Åkesson, P., Cooney, J., Kishimoto, F. & Björck, L. Protein H--a novel IgG binding
635 bacterial protein. *Mol. Immunol.* **27,** 523–531 (1990).
636 11. Pawel-Rammingen, von, U., Johansson, B. P. & Björck, L. IdeS, a novel streptococcal
637 cysteine proteinase with unique specificity for immunoglobulin G. *EMBO J* **21,** 1607–
638 1615 (2002).
639 12. Collin, M. & Olsén, A. EndoS, a novel secreted protein from *Streptococcus pyogenes*
640 with endoglycosidase activity on human IgG. *EMBO J* **20,** 3046–3055 (2001).
641 13. Subedi, G. P. & Barb, A. W. The structural role of antibody N-glycosylation in
642 receptor interactions. *Structure* **23,** 1573–1583 (2015).
643 14. Subedi, G. P. & Barb, A. W. The immunoglobulin G1 N-glycan composition affects
644 binding to each low affinity Fc γ receptor. *Mabs* **8,** 1512–1524 (2016).

645 15. Burton, D. R. Immunoglobulin G: functional sites. *Mol. Immunol.* **22,** 161–206 (1985).
646 16. Burton, D. R. & Dwek, R. A. Immunology. Sugar determines antibody activity.
647 *Science* **313,** 627–628 (2006).
648 17. Shinkawa, T. *et al.* The absence of fucose but not the presence of galactose or
649 bisecting N-acetylglucosamine of human IgG1 complex-type oligosaccharides shows
650 the critical role of enhancing antibody-dependent cellular cytotoxicity. *J. Biol. Chem.*
651 **278,** 3466–3473 (2003).
652 18. Okazaki, A. *et al.* Fucose depletion from human IgG1 oligosaccharide enhances
653 binding enthalpy and association rate between IgG1 and FcgammaRIIIa. *J. Mol. Biol.*
654 **336,** 1239–1249 (2004).
655 19. Peschke, B., Keller, C. W., Weber, P., Quast, I. & Lünemann, J. D. Fc-galactosylation
656 of human immunoglobulin gamma isotypes improves C1q binding and enhances
657 complement-dependent cytotoxicity. *Front Immunol* **8,** 646 (2017).
658 20. Lux, A., Yu, X., Scanlan, C. N. & Nimmerjahn, F. Impact of immune complex size
659 and glycosylation on IgG binding to human FcγRs. *J. Immunol.* **190,** 4315–4323
660 (2013).
661 21. Nose, M. & Wigzell, H. Biological significance of carbohydrate chains on monoclonal
662 antibodies. *Proc. Natl. Acad. Sci. U.S.A.* **80,** 6632–6636 (1983).
663 22. Alter, G. *et al.* High-resolution definition of humoral immune response correlates of
664 effective immunity against HIV. *Mol. Syst. Biol.* **14,** e7881 (2018).
665 23. Lu, L. L. *et al.* A Functional Role for Antibodies in Tuberculosis. *Cell* **167,** 433–
666 443.e14 (2016).
667 24. Allhorn, M., Olin, A. I., Nimmerjahn, F. & Collin, M. Human IgG/Fc gamma R
668 interactions are modulated by streptococcal IgG glycan hydrolysis. *PLoS ONE* **3,**
669 e1413 (2008).
670 25. Collin, M. *et al.* EndoS and SpeB from *Streptococcus pyogenes* inhibit
671 immunoglobulin-mediated opsonophagocytosis. *Infect. Immun.* **70,** 6646–6651 (2002).
672 26. Sjögren, J., Okumura, C. Y. M., Collin, M., Nizet, V. & Hollands, A. Study of the IgG
673 endoglycosidase EndoS in group A streptococcal phagocyte resistance and virulence.
674 *BMC Microbiol.* **11,** 120 (2011).
675 27. Picotti, P. & Aebersold, R. Selected reaction monitoring-based proteomics: workflows,
676 potential, pitfalls and future directions. *Nat Meth* **9,** 555–566 (2012).
677 28. Anderson, L. & Hunter, C. L. Quantitative mass spectrometric multiple reaction
678 monitoring assays for major plasma proteins. *Mol. Cell Proteomics* **5,** 573–588 (2006).
679 29. Addona, T. A. *et al.* Multi-site assessment of the precision and reproducibility of
680 multiple reaction monitoring-based measurements of proteins in plasma. *Nat.*
681 *Biotechnol.* **27,** 633–641 (2009).
682 30. Hong, Q., Lebrilla, C. B., Miyamoto, S. & Ruhaak, L. R. Absolute quantitation of
683 immunoglobulin G and its glycoforms using multiple reaction monitoring. *Anal. Chem.*
684 **85,** 8585–8593 (2013).
685 31. Collin, M., Shannon, O. & Björck, L. IgG glycan hydrolysis by a bacterial enzyme as a
686 therapy against autoimmune conditions. *Proc. Natl. Acad. Sci. U.S.A.* **105,** 4265–4270
687 (2008).
688 32. Sjögren, J. *et al.* EndoS and EndoS2 hydrolyze Fc-glycans on therapeutic antibodies
689 with different glycoform selectivity and can be used for rapid quantification of high-
690 mannose glycans. *Glycobiology* **25,** 1053–1063 (2015).
691 33. Dixon, E. V. *et al.* Fragments of bacterial endoglycosidase s and immunoglobulin g
692 reveal subdomains of each that contribute to deglycosylation. *J. Biol. Chem.* **289,**
693 13876–13889 (2014).
694 34. Collin, M. & Olsén, A. EndoS, a novel secreted protein from *Streptococcus pyogenes*

695 with endoglycosidase activity on human IgG. *EMBO J* **20,** 3046–3055 (2001).
696 35. Pucić, M. *et al.* High throughput isolation and glycosylation analysis of IgG-variability
697 and heritability of the IgG glycome in three isolated human populations. *Mol. Cell*
698 *Proteomics* **10,** M111.010090 (2011).
699 36. Wuhrer, M. *et al.* Glycosylation profiling of immunoglobulin G (IgG) subclasses from
700 human serum. *Proteomics* **7,** 4070–4081 (2007).
701 37. Karlsson, C. A. Q. *et al. Streptococcus pyogenes* infection and the human proteome
702 with a special focus on the IgG-cleaving enzyme IdeS. *Mol. Cell Proteomics*
703 mcp.RA117.000525 (2018). doi:10.1074/mcp.RA117.000525
704 38. Centor, R. M., Witherspoon, J. M., Dalton, H. P., Brody, C. E. & Link, K. The
705 diagnosis of strep throat in adults in the emergency room. *Med. Decis. Making* **1,** 239–
706 246 (1981).
707 39. Allhorn, M., Olsén, A. & Collin, M. EndoS from *Streptococcus pyogenes* is
708 hydrolyzed by the cysteine proteinase SpeB and requires glutamic acid 235 and
709 tryptophans for IgG glycan-hydrolyzing activity. *BMC Microbiol.* **8,** 3 (2008).
710 40. Nandakumar, K. S., Johansson, B. P., Björck, L. & Holmdahl, R. Blocking of
711 experimental arthritis by cleavage of IgG antibodies in vivo. *Arthritis Rheum.* **56,**
712 3253–3260 (2007).
713 41. Albert, H., Collin, M., Dudziak, D., Ravetch, J. V. & Nimmerjahn, F. In vivo
714 enzymatic modulation of IgG glycosylation inhibits autoimmune disease in an IgG
715 subclass-dependent manner. *Proc. Natl. Acad. Sci. U.S.A.* **105,** 15005–15009 (2008).
716 42. Trastoy, B. *et al.* Crystal structure of *Streptococcus pyogenes* EndoS, an
717 immunomodulatory endoglycosidase specific for human IgG antibodies. *Proc. Natl.*
718 *Acad. Sci. U.S.A.* **111,** 6714–6719 (2014).
719 43. Benkhoucha, M. *et al.* IgG glycan hydrolysis by EndoS inhibits experimental
720 autoimmune encephalomyelitis. *J. Neuroinflammation* **9,** 209 (2012).
721 44. Sjögren, J. *et al.* EndoS2 is a unique and conserved enzyme of serotype M49 group A
722 *Streptococcus* that hydrolyses N-linked glycans on IgG and alpha1-acid glycoprotein.
723 *Biochem. J.* **455,** 107–118 (2013).
724 45. Nord, C. E., Linder, L., Wadström, T. & Lindberg, A. A. Formation of glycoside-
725 hydrolases by oral streptococci. *Arch. Oral Biol.* **18,** 391–402 (1973).
726 46. Shelburne, S. A. *et al.* A combination of independent transcriptional regulators shapes
727 bacterial virulence gene expression during infection. *PLoS Pathog* **6,** e1000817 (2010).
728 47. Collin, M. & Olsén, A. Effect of SpeB and EndoS from *Streptococcus pyogenes* on
729 human immunoglobulins. *Infect. Immun.* **69,** 7187–7189 (2001).
730 48. Shelburne, S. A. *et al.* A direct link between carbohydrate utilization and virulence in
731 the major human pathogen group A *Streptococcus*. *Proc. Natl. Acad. Sci. U.S.A.* **105,**
732 1698–1703 (2008).
733 49. Bao, Y.-J. *et al.* CovRS-regulated transcriptome analysis of a hypervirulent M23 strain
734 of group A *Streptococcus pyogenes* provides new insights into virulence determinants.
735 *J. Bacteriol.* **197,** 3191–3205 (2015).
736 50. Lancefield, R. C. Differentiation of group A streptococci with a common R antigen
737 into three serological types, with special reference to the bactericidal test. *J. Exp. Med.*
738 **106,** 525–544 (1957).
739 51. Panda, S., Zhang, J., Tan, N. S., Ho, B. & Ding, J. L. Natural IgG antibodies provide
740 innate protection against ficolin-opsonized bacteria. *EMBO J* **32,** 2905–2919 (2013).
741 52. Norrby-Teglund, A., Ihendyane, N. & Darenberg, J. Intravenous immunoglobulin
742 adjunctive therapy in sepsis, with special emphasis on severe invasive group A
743 streptococcal infections. *Scand. J. Infect. Dis.* **35,** 683–689 (2003).
744 53. Alejandria, M. M., Lansang, M. A. D., Dans, L. F. & Mantaring, J. B. Intravenous

745 immunoglobulin for treating sepsis, severe sepsis and septic shock. *Cochrane*
746 *Database Syst. Rev.* CD001090 (2013). doi:10.1002/14651858.CD001090.pub2
747 54. Kaul, R. *et al.* Intravenous immunoglobulin therapy for streptococcal toxic shock
748 syndrome--a comparative observational study. The Canadian Streptococcal Study
749 Group. *Clin. Infect. Dis.* **28,** 800–807 (1999).
750 55. Darenberg, J. *et al.* Intravenous immunoglobulin G therapy in streptococcal toxic
751 shock syndrome: a European randomized, double-blind, placebo-controlled trial. *Clin.*
752 *Infect. Dis.* **37,** 333–340 (2003).
753 56. Kaul, R., McGeer, A., Low, D. E., Green, K. & Schwartz, B. Population-based
754 surveillance for group A streptococcal necrotizing fasciitis: Clinical features,
755 prognostic indicators, and microbiologic analysis of seventy-seven cases. Ontario
756 Group A Streptococcal Study. *Am. J. Med.* **103,** 18–24 (1997).
757 57. Norrby-Teglund, A. *et al.* Plasma from patients with severe invasive group A
758 streptococcal infections treated with normal polyspecific IgG inhibits streptococcal
759 superantigen-induced T cell proliferation and cytokine production. *J. Immunol.* **156,**
760 3057–3064 (1996).
761 58. Skansén-Saphir, U., Andersson, J., Björk, L. & Andersson, U. Lymphokine production
762 induced by streptococcal pyrogenic exotoxin-A is selectively down-regulated by
763 pooled human IgG. *Eur. J. Immunol.* **24,** 916–922 (1994).
764 59. Andersson, U., Björk, L., Skansén-Saphir, U. & Andersson, J. Pooled human IgG
765 modulates cytokine production in lymphocytes and monocytes. *Immunol. Rev.* **139,**
766 21–42 (1994).
767 60. Collin, M. & Fischetti, V. A. A novel secreted endoglycosidase from *Enterococcus*
768 *faecalis* with activity on human immunoglobulin G and ribonuclease B. *J. Biol. Chem.*
769 **279,** 22558–22570 (2004).
770 61. Muramatsu, H. *et al.* Molecular cloning and expression of endo-beta-N-
771 acetylglucosaminidase D, which acts on the core structure of complex type asparagine-
772 linked oligosaccharides. *J. Biochem.* **129,** 923–928 (2001).
773 62. Shadnezhad, A. *et al.* EndoSd: an IgG glycan hydrolyzing enzyme in *Streptococcus*
774 *dysgalactiae* subspecies *dysgalactiae*. *Future Microbiol*. **11,** 721–736 (2016).
775 63. Flock, M., Frykberg, L., Sköld, M., Guss, B. & Flock, J.-I. Antiphagocytic function of
776 an IgG glycosyl hydrolase from Streptococcus equi subsp. equi and its use as a vaccine
777 component. *Infect. Immun.* **80,** 2914–2919 (2012).
778 64. Malmström, E. *et al.* Large-scale inference of protein tissue origin in gram-positive
779 sepsis plasma using quantitative targeted proteomics. *Nat. Comms.* **7,** 10261 (2016).
780 65. Lange, V., Picotti, P., Domon, B. & Aebersold, R. Selected reaction monitoring for
781 quantitative proteomics: a tutorial. *Mol. Syst. Biol.* **4,** 222 (2008).
782 66. MacLean, B. *et al.* Skyline: an open source document editor for creating and analyzing
783 targeted proteomics experiments. *Bioinformatics* **26,** 966–968 (2010).
784 67. MacLean, B. *et al.* Effect of collision energy optimization on the measurement of
785 peptides by selected reaction monitoring (SRM) mass spectrometry. *Anal. Chem.* **82,**
786 10116–10124 (2010).
787 68. Collin, M. & Olsén, A. Generation of a mature streptococcal cysteine proteinase is
788 dependent on cell wall-anchored M1 protein. *Mol. Microbiol.* **36,** 1306–1318 (2000).
789 69. Walker, M. J. *et al.* DNase Sda1 provides selection pressure for a switch to invasive
790 group A streptococcal infection. *Nat. Med.* **13,** 981–985 (2007).
791 70. Fiebig, A. *et al.* Comparative genomics of *Streptococcus pyogenes* M1 isolates
792 differing in virulence and propensity to cause systemic infection in mice. *Int. J. Med.*
793 *Microbiol.* **305,** 532–543 (2015).
794 71. Påhlman, L. I. *et al.* Streptococcal M protein: a multipotent and powerful inducer of

795 inflammation. *J. Immunol.* **177,** 1221–1228 (2006).
796 72. Shannon, O. *et al.* Severe streptococcal infection is associated with M protein-induced
797 platelet activation and thrombus formation. *Mol. Microbiol.* **65,** 1147–1157 (2007).
798
799

800 # Figures

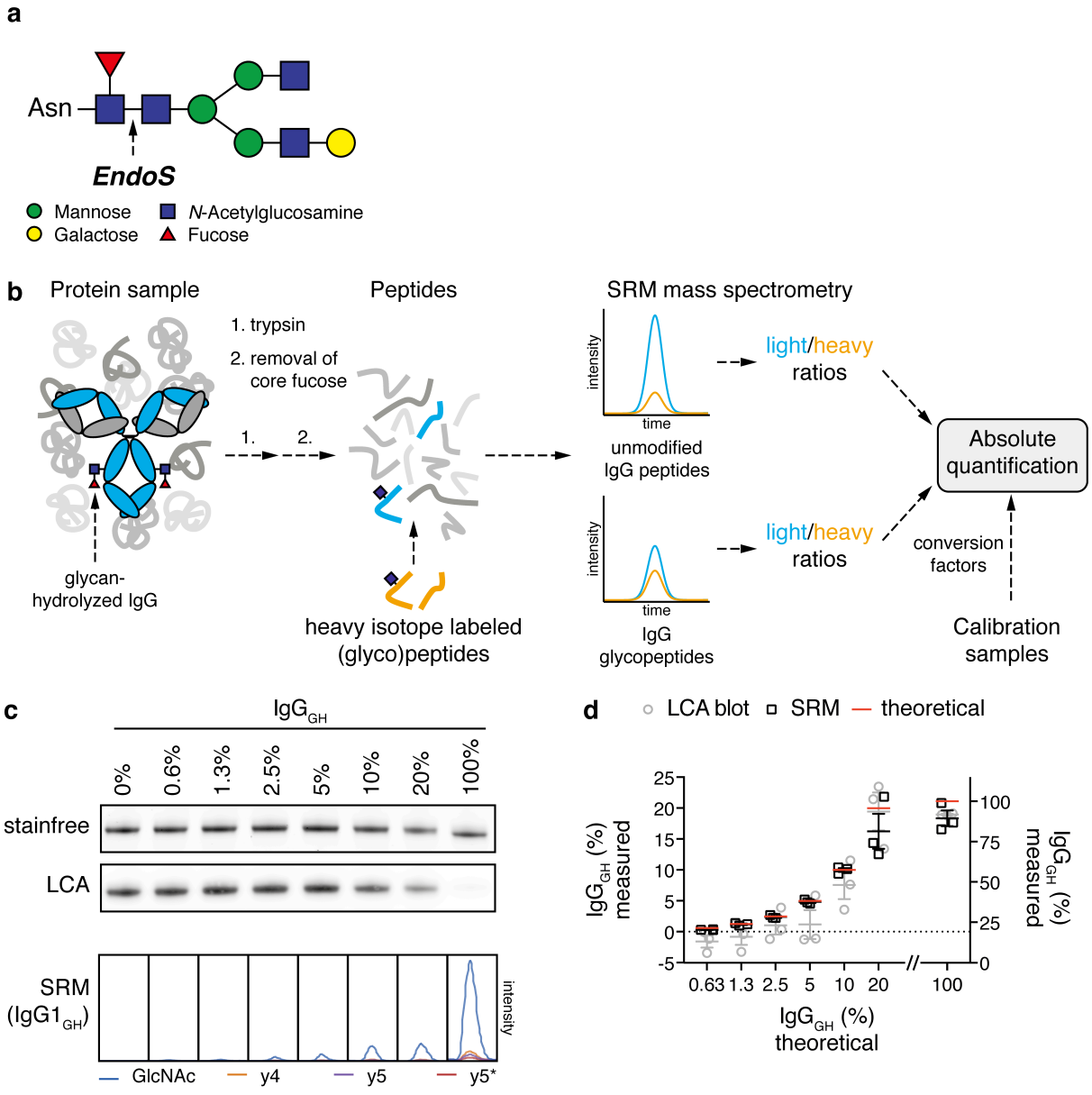

801

802 FIGURE 1: TARGETED MASS SPECTROMETRY TO QUANTIFY IGG GLYCAN HYDROLYSIS

803 a) Typical *N*-glycan structure found on N297 of human IgG antibodies. The arrow marks the
804 EndoS cleavage site in the chitobiose core of the glycan. The EndoS reaction product is an
805 IgG carrying either a single GlcNAc or a GlcNAc-Fucose disaccharide, depending on the
806 core fucosylation status of the antibody.

807 b) Overview of the SRM-MS method. Complex protein samples are digested to peptides
808 using trypsin and potential core fucosylation is removed using α-fucosidase. The resulting
809 peptide samples are spiked with heavy isotope labeled (glyco)peptide standards
810 corresponding to both subclass specific IgG glycopeptides modified with a single GlcNAc

811 residue as well as subclass specific unmodified peptides. This peptide mixture is analyzed by
812 SRM mass spectrometry resulting in light/heavy ratios for each of the peptides of interest.
813 The absolute amount (concentration) of each IgG subclass as well as the amount of IgG_{GH} is
814 derived from the obtained ratios, using conversion factors determined from a defined set of
815 standard samples

816 c&d) Validation of SRM-MS quantitative accuracy. A set of plasma samples with defined
817 percentages of IgG_{GH} was prepared by dilution of EndoS-treated plasma with untreated
818 control plasma. The samples were analyzed separately in triplicate by SDS-PAGE/LCA
819 blotting and SRM mass spectrometry. Raw data from both methods is shown in panel c. For
820 the SRM method the chromatograms originating from the glycan-hydrolyzed IgG1
821 glycopeptide are shown, each transition in a different color. The asterisk denotes a fragment
822 ion that has undergone a neutral loss of the GlcNAc modification. The degree of IgG glycan
823 hydrolysis in the standard sample set was quantified using both methods (panel d). The red
824 line marks the theoretical value and the measured values are depicted in grey circles (LCA
825 blot) and black boxes (SRM) respectively. The means and standard errors are plotted and
826 each individual data point is marked with a circle or box. The first 6 values are plotted on the
827 left z-axis, the final 100% IgG_{GH} sample on the right y-axis.

828

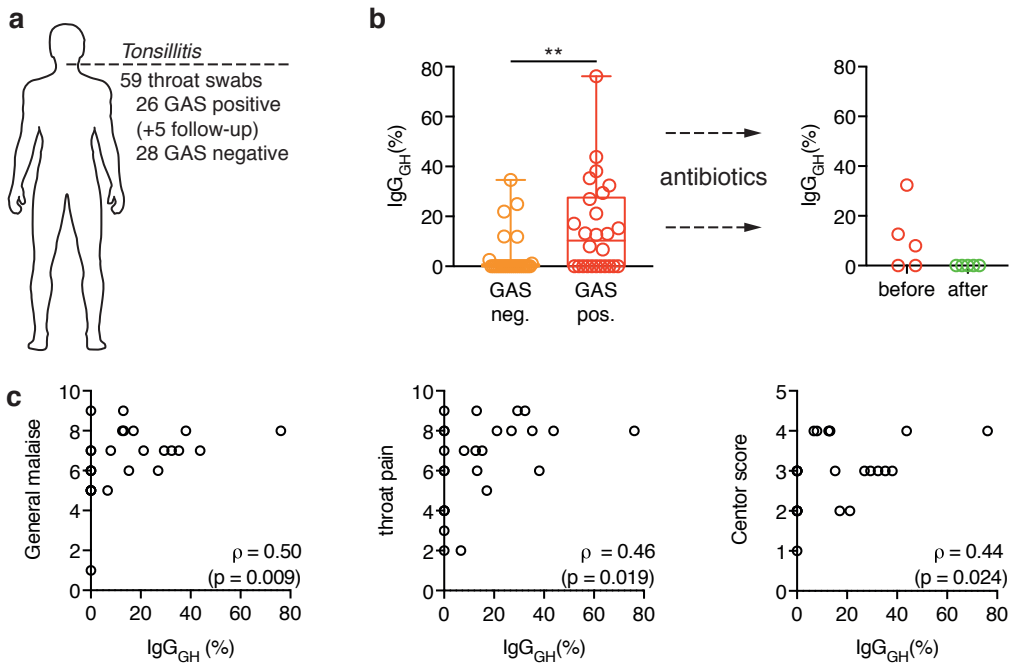

FIGURE 2: IGG GLYCAN HYDROLYSIS DURING GAS TONSILLITITS

a) Overview of the collected throat swab samples from patients seeking medical attention for a sore throat. A total of 59 samples were taken from 54 different patients (26 GAS positive tonsillitis, 28 GAS negative tonsillitis). Follow-up refers to additional samples that were taken from 5 of the GAS tonsillitis patients after antibiotic treatment.

b) Percentage of glycan-hydrolyzed IgG as determined by SRM-MS analysis of tonsillar swabs from patients with, either GAS-negative (orange) or GAS-positive (red) tonsillitis. The boxes represent the 25th to 75th percentile with the median depicted as a line in the middle. The whiskers reach from the smallest to the largest data point, all of which are marked as circles. Glycan hydrolysis of the individual subclasses is shown in table S4. The glycopeptides from IgG3 and IgG4 could not be measured in these samples due to interfering background and were omitted from this analysis. Data was analyzed using a Mann-Whitney test (Table S6) (ns: $p>0.05$, **: $p<0.01$).

c) The tonsillitis patients were asked to grade their a general malaise (left) and throat pain (middle) on a scale from 0-10 and the centor score[38] (right) was determined. These parameters were correlated to the IgG glycan hydrolysis measured in tonsillar swabs using SRM-MS. Correlation was analyzed according to Spearman (Table S7).

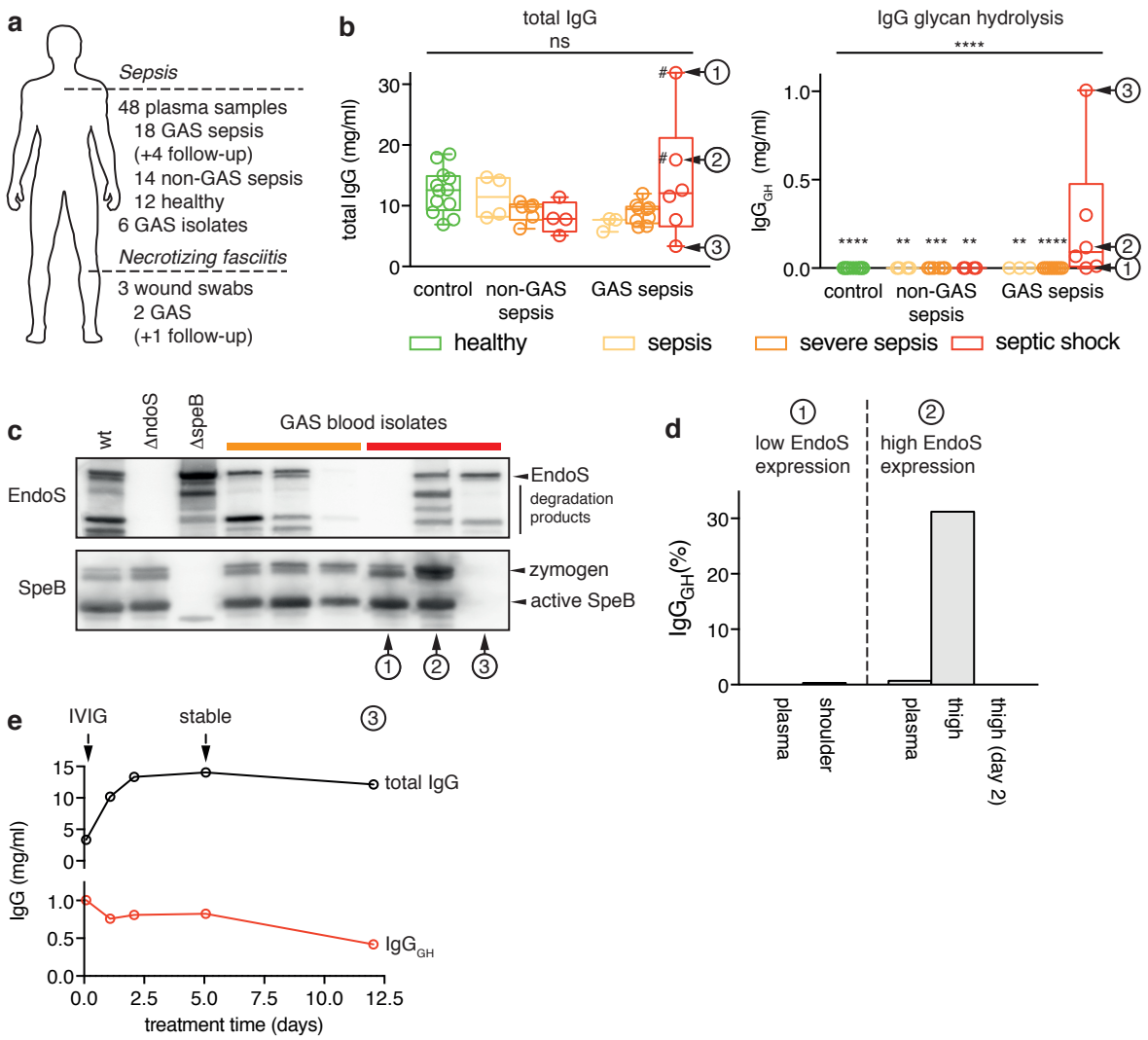

848

849 FIGURE 3: IGG GLYCAN HYDROLYSIS DURING INVASIVE GAS INFECTION

850 a) Overview of the collected samples from sepsis patients. A total of 48 plasma samples, 3
851 wound swabs and 6 GAS isolates was collected from 32 patients (18 GAS sepsis, 14 non-
852 GAS sepsis) and 12 healthy control individuals. Follow-up refers to 4 additional plasma
853 samples that were taken from the same patient during the course of treatment and recovery.

854 b) Plasma concentration of total IgG (left panel) as well as the glycan-hydrolyzed IgG (right
855 panel) as determined by SRM-MS. The patients are grouped according to infection state
856 (healthy, non-GAS sepsis, GAS sepsis), as well as sub-grouped according to severity of
857 disease (sepsis, severe sepsis, septic shock). The boxes represent the 25th to 75th percentile
858 with the median depicted as a center line. The whiskers reach from the smallest to the largest
859 data point, all of which are marked as circles. Glycan hydrolysis of the individual subclasses
860 is shown in table S5. The p-value of the overall comparison of all the groups (by Kruskal-
861 Wallis test) as well as adjusted p-values for the individual comparisons of the GAS septic

862 shock group with each of the other groups are depicted (ns: $p>0.05$, *: $p<0.05$, **: $p<0.01$,
863 ***: $p<0.001$, ****: $p<0.0001$). For a more detailed description of the statistical analysis see
864 tables S8&S9). Two patients (marked by the hashtag #) had received IVIG treatment before
865 the sample was drawn, affecting their total IgG concentrations. From three patients (marked
866 1-3) additional samples could be obtained and their analysis is shown in the other panels of
867 this figure.

868 c) Expression of EndoS and SpeB by clinical GAS isolates *in vitro*. Blood culture isolates
869 from patients 1-3 as well as three patients from the GAS severe sepsis group were analyzed
870 with respect to their ability of secrete EndoS (top panel) and SpeB (bottom panel) into the
871 culture supernatant *in vitro*. The culture supernatants were analyzed by SDS-PAGE followed
872 by immunoblotting using rabbit antisera specific to EndoS and SpeB respectively. AP1 (wt)
873 and isogenic *ndoS* and *speB* mutants were used as positive and negative controls respectively.

874 d) Local vs. systemic glycan hydrolysis. From patients 1 & 2, wound swab samples from the
875 site of infection (patient 1: shoulder and patient 2: thigh) could be obtained and were
876 analyzed by SRM-MS. The percentage of IgG_{GH} in the tissue as well as in plasma is shown.

877 e) IgG glycan hydrolysis over the course of infection. A series of plasma samples from
878 patient 3 (starting at 2h after admission until 12 days later) was analyzed using SRM-MS.
879 Both the concentration of total IgG (black) as well as IgG_{GH}(red) is shown. The arrows mark
880 onset of IVIG treatment (4h) and the time point when the patient was stable (5 days).

881

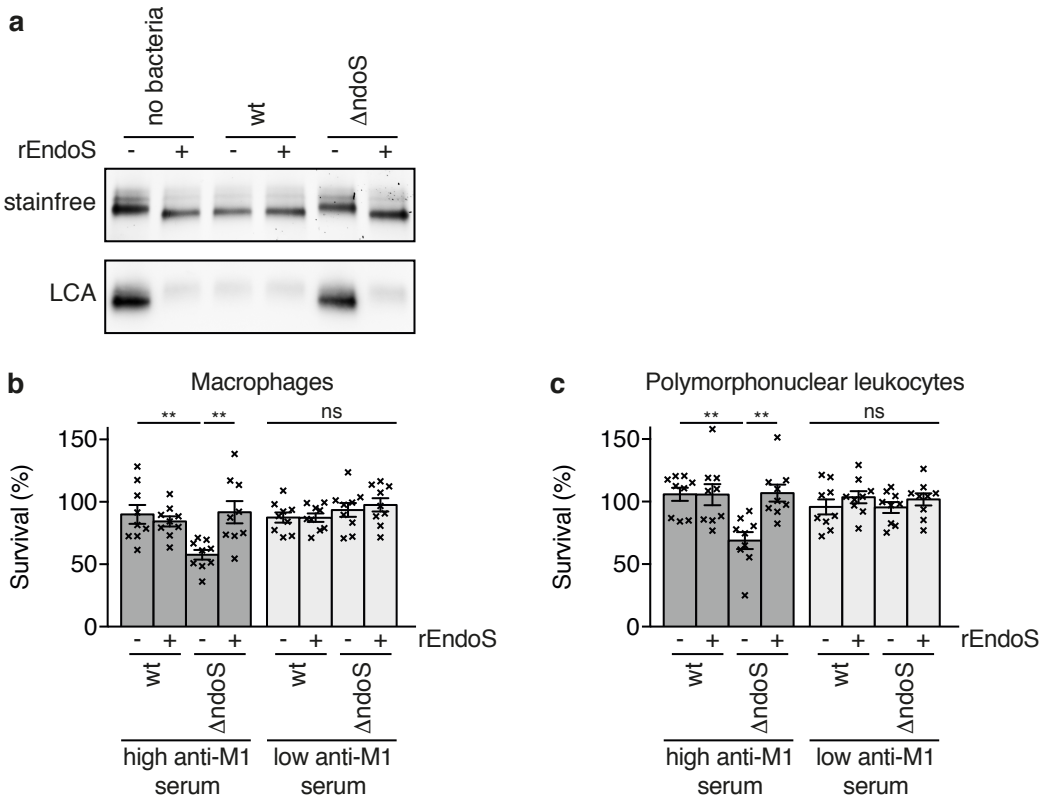

FIGURE 4: ENDOS CONFERS RESISTANCE TO PHAGOCYTIC KILLING

a) GAS 5448 and an isogenic *ndoS* mutant were grown in human saliva supplemented with 5% human serum. IgGs were purified by Protein G and analyzed by SDS-PAGE (top) and LCA blot (bottom). Addition of recombinant EndoS (rEndoS) was used to complement the mutation.

b) Saliva-grown GAS 5448 and an isogenic *ndoS* mutant were challenged with human monocyte-derived macrophages (left) and human polymorphonuclear leukocytes (right) in the presence of serum with a high (dark grey) or low (light grey) anti-M1 IgG response. Survival rates were determined by numerating bacteria both in the initial inoculum as well as after incubation with the phagocytic cells. Data from 3 independent experiments with different cell donors (each preformed in triplicate, total n=9) was combined and analyzed using a Kruskal-Wallis test followed by Dunn´s multiple comparison test (Tables S10-13) (ns: $p>0.05$, **: $p<0.01$). The bar represents the mean, with the standard error depicted as error bars. Each individual data point is represented with a cross, showing the variability between the individual experiments and the replicates within the same experiment.

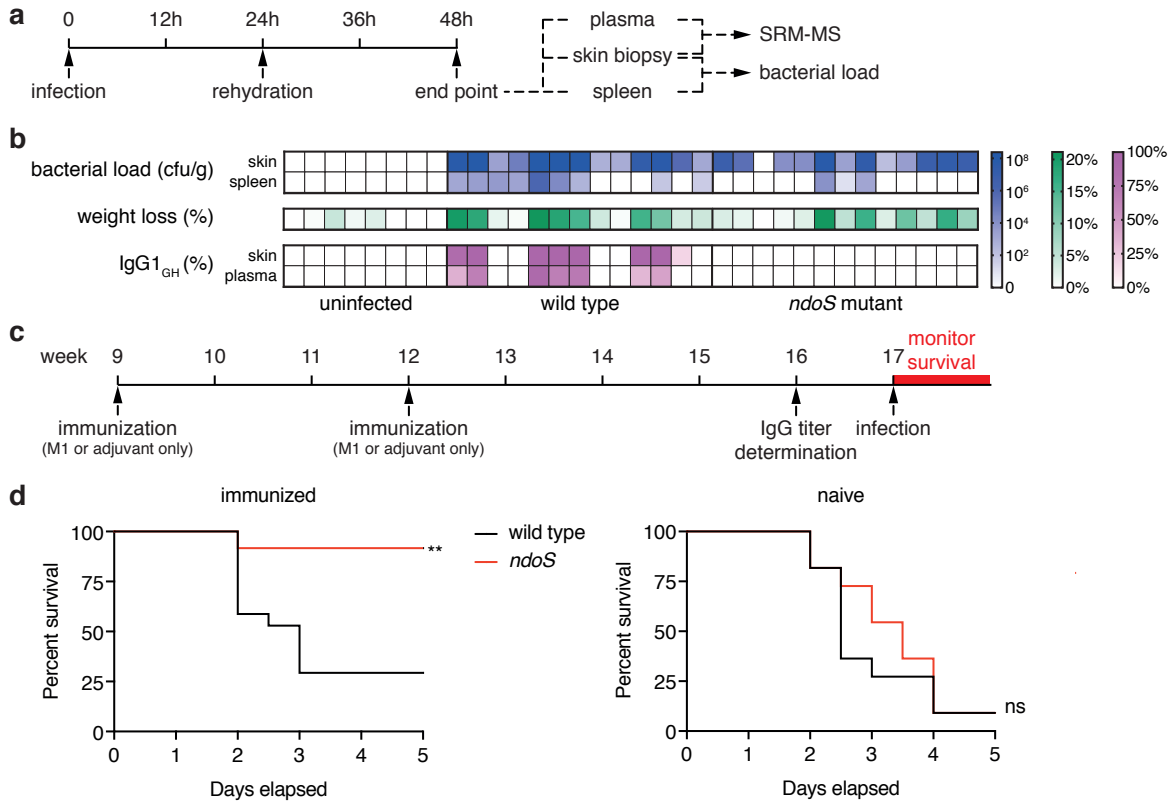

FIGURE 5: ENDOS LEADS TO IGG GLCYANS HYDROLYSIS AND CONFERS A SELECTIVE ADVANTAGE IN A MOUSE MODEL OF GAS INFECTION

a) Experimental setup for the infections of immunologically naïve mice. 9 week old, female C57BL/6 mice were infected subcutaneously in the flank with GAS AP1, an *ndoS* mutant or PBS. The animals were rehydrated by injection of 0.5 ml saline at 24 h and sacrificed at 48 h post infection. The spleen and a skin biopsy from the site of injection were taken to assess bacterial loads and the skin sample, as well as a plasma sample were used for analysis by SRM-MS.

b) Bacterial load (blue), weight loss (green) and percentage of IgG1 glycan hydrolysis as determined by SRM-MS (purple) at 48h post infection. Each column corresponds to an individual animal.

c) Experimental setup for the immunization with M1 and subsequent infection of mice. 9 week old, female C57BL/6 mice were injected with purified M1 protein or adjuvant only and received a second dose at 12 weeks of age. After 4 weeks, the anti-M1 IgG response was assessed by ELISA and the animals were infected subcutaneously one week later.

d) Survival of M1-immunized (right) and mock-immunized (left) animals after infection with either GAS AP1 wild-type (black) or *ndoS* mutant (red). Mice were monitored twice

917 daily for survival for a period of 5 days. Curves were compared using a Mantel-Cox test (ns:
918 $p>0.05$, **: $p<0.01$).

919